Optical Loss Analysis of PV Modules

Conference Paper · June 2016

DOI: 10.4229/EUPVSEC20162016-2BV.7.60

3 authors:


Malcolm Abbott
PV Lighthouse


Keith McIntosh
PV Lighthouse


Ben Sudbury
PV Lighthouse

OPTICAL LOSS ANALYSIS OF PV MODULES

Malcolm Abbott, Keith McIntosh and Ben Sudbury

PV Lighthouse, Coledale, NSW 2515, Australia

ABSTRACT: Photovoltaic modules present a complex system of interactions between various optical materials and the solar cells. Understanding how this system operates optically is an important part of designing modules with high output power. This paper demonstrates how simulations based on a combination of Monte Carlo ray tracing and thin film optics can be used to determine the optical loses in photovoltaic cells and modules. It finds that the performance of commercial cells and modules can be reproduced allowing a detailed loss analysis of the optics to be determined. Various examples are given on the use of such a simulation approach, including an assessment of the module performance as a function of cell spacing, rear surface lambertian fraction and optimization of front surfaces under encapsulation.

1 INTRODUCTION

Minimizing cell-to-module losses is vital to achieving modules with high output power. This task is made very difficult due to the complex combination of different materials, thin film optics, surface geometries and the various interactions with the active device. Simulation software can play an important role in helping to characterize these interactions, assess the loss mechanisms and ultimately optimize the module design. There are many well developed software tools to simulate the performance of photovoltaic cells, however for modules there are many less options and those that are available tend to be slow and difficult to use.

Recently, PV Lighthouse [1] introduced a new software tool specifically designed to simulate the optical performance of photovoltaic modules. Through optimisation of the algorithms, combined with the scalable processing power of cloud computing, the solving is extremely fast allowing many variations of the module layers to be rapidly simulated. This paper discusses some of the fundamental principles of this approach and demonstrates how it may be used to assess the optical losses for a particular module design as well as to understand the sensitivity of different aspects to the overall performance.

2. RAY TRACING BASELINE MODULES

The simulation method used in this work is based on a combination of ray tracing and thin film optics. A Monte Carlo approach is employed in which random numbers are used to determine both the initialization and progression of rays of a particular wavelength through the system of optical materials. As they interact with interfaces where thin films are present the transfer matrix method is used to solve the reflection, absorption and transmission (RAT) of the beam [2]. Interfaces can also be defined more simply as having particular RAT properties. In both cases a Lambertian scattering model can be employed. Surface texturing is accounted for using a variety of geometric surface morphologies implemented as unit cells. The random nature of certain textures is handled through random shifts in the beam position during entry and exit to the unit cell. A more detailed description of this approach, as well as a comparison to experimental results, has recently been presented [3].

The impact of metal contacts (fingers, busbars and coatings) was not included in the version of the MRT used in this work. Where it was relevant the final value of Jsc presented was scaled based on the percentage of shading, taking into account the effective shading width [10]. It should be noted that more recent versions of the MRT include the ability to simulate all types of common metal contact patterns, including special busbar alternatives such as the so called MultiWire approach. Results on some of these types of simulation were presented at this conference [4].

2.1 Baseline module performance

There are many different flavours of multicrystalline cells and modules currently on the market. To get an estimate of the most common performance and design parameters we conducted a survey of publically available datasheets (cells and modules) from a selection of commercial manufacturers. Here we focus on the data related to standard screen print cells fabricated on multi-crystalline substrates. Rather than quote every exact source of this data, we keep the manufacturer names anonymous and refer the reader instead to the ENF database where all datasheets were sourced [5]. Roughly half of the data was from tier 1 manufacturers, the rest were tier 2 and 3. The summary of the I_{sc} (Figure 1) reveals an average value of 8.75 A for the cells and 9.05 A (per cell) for modules. This gain in current for the modules is expected and is due to several factors including collection of carriers from outside the cell area and enhanced trapping of light initially reflected from metal fingers and isotexture.

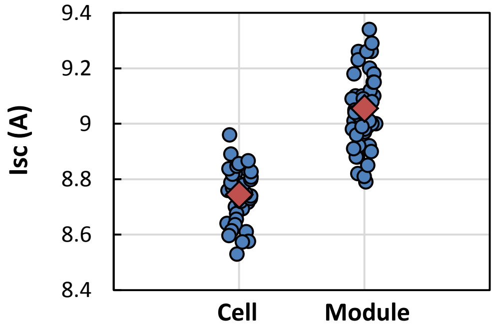

Figure 1: Short circuit current (Isc) for cells and modules as reported by a variety of manufacturers datasheets.

The basic inputs for the material and geometric parameters of the cells and modules were also extracted from the data sheets. In this case there was significantly more error since the exact material properties cannot be known and would be expected to vary between products. Further work is required to establish common values for these more accurately; however for the purposes of this work the values used (Table 1) were a reasonable approximation. Note the use of a front-side AR coating on the glass which we found to be very common on the manufacturers datasheets.

Table I. Simulation inputs for baseline module

Location	Property	Value
Front glass	Thickness	3.2 mm
	Material	Borofloat33
	AR coat	Enki cleanARC
EVA	Thickness	450 µm
	Material	[6]
Cell bulk	Thickness	180 µm
	Material	[8]
Cell texture	Type	Inverted caps
	Angle	60°
	Height	4 µm
Cell ARC	Thickness	75 nm
	Material	SiNx (2.03) [7]
Cell rear	Reflection	65%
	Absorption	35%
	Lamb. fraction	70%
Cell layout	spacing	0.2 mm
Backsheet	Reflection	85%
	Absorption	15%
	Lamb. fraction	50%

Conversion of an optical generation current into collected cell current required wavelength dependent collection efficiency data (CE). This was generated using PC1D with common front, bulk and rear recombination inputs [9] and 100% internal reflection (to remove impact of light trapping). The MRT software allows this CE to be entered as an input, resulting in an EQE curve and cell Jsc as outputs.

The results for the baseline module under standard test conditions are shown in Table 2 and Figure 2. The optical losses have been grouped by material where EVA includes the surrounding area of the cell. Weighting these losses via the AM1.5G spectrum allows them to be expressed in terms of a generation current (Table 2). The error in the current is the calculated 95% confidence interval based on the set of results from 200 different simulation runs of 5000 rays.

Table 2. Optical losses simulated for the baseline module

	Mean (mA/cm²)	Fraction of Jinc (%)
Incident	46.71	100
Reflected – external	1.13 ±0.017	2.41
Reflected – escape	1.82 ±0.015	3.89
Absorption glass	0.57 ±0.001	1.23
Absorption EVA	1.05 ±0.003	2.26
Absorption in SiNx	0.11 ±0.000	0.25
Absorption in Si	37.71 ±0.023	80.7
Absorption in Al rear	4.12 ±0.007	8.81
Absorption in backsheet	0.19 ±0.002	0.42

The wavelength dependent reflection and absorption for this baseline module reveals which parts of the spectrum are lost in the different layers. At very short wavelengths over 80% of the light was absorbed in the EVA. For longer wavelengths the absorption at the rear of the solar cell was significant.

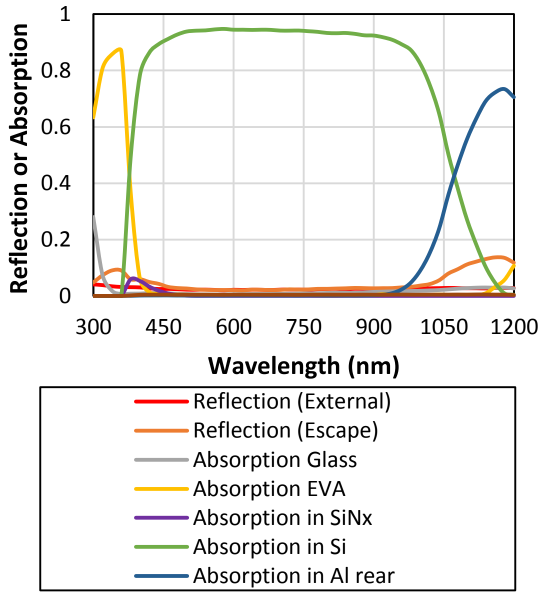

Figure 2: Wavelength dependent reflection and absorption losses simulated for the baseline module without metalisation.

After applying the collection efficiency and accounting for the metal shading, the simulated current of the cell was 8.8 A with no encapsulation and 9.0 A when incorporated into a module unit cell. This agrees well with the data shown in Figure 1 for the commercially available cells and modules. With so many free variables it is hardly surprising that we were able to reproduce these numbers. However, it is encouraging that the output of the simulator is in the correct range and for the purposes of this paper our baseline module can be used to demonstrate the power and versatility of the simulation approach.

2.2 Improving the confidence interval

Inherent to the Monte Carlo approach of ray tracing is the need to define the number of rays to trace as well as the maximum number of interaction with interfaces. Lower numbers lead to faster simulations but with less accurate results. To demonstrate this effect we simulated the baseline module several times and employed the sweeping feature of the MRT to vary the maximum number of rays for each simulation. The results are plotted in Figure 3 in terms of absolute current for each run as well as the 95% confidence interval. From the data it is clear that increasing the number of simulated rays improves the accuracy of the result. However, it is interesting to note that with even relatively few rays (here the minimum used was 30,000) the final value of current from the solar cell was within 30 mA (0.12 mA/cm^2) of the more accurate value achieved with 1 million rays. If speed of simulation is required then this level of error may be acceptable.

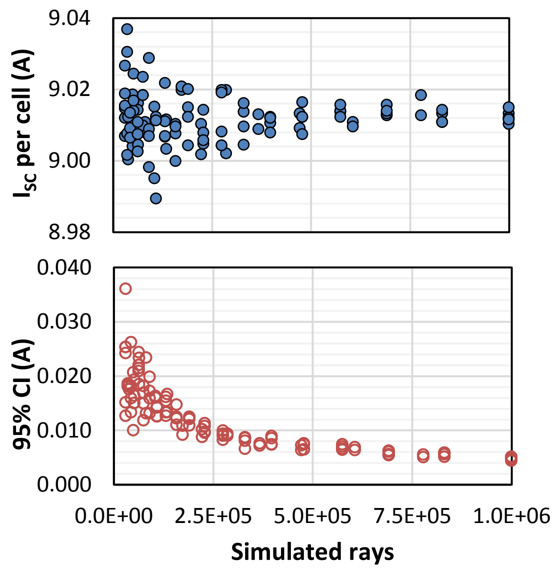

Figure 3: Impact of the total number of rays simulated on (top) the total module collected current per cell and (bottom) on the 95% confidence interval.

2.3 Angular dependences of losses

Modules in the field experience a variety of incident angles of the incoming light. To study the performance of a module design as the sun moves across the sky we simply sweep the zenith angle. In doing so the overall incident intensity of the light is reduced, as such it is instructive to present the results both in absolute terms and as a percentage of the incoming light intensity.

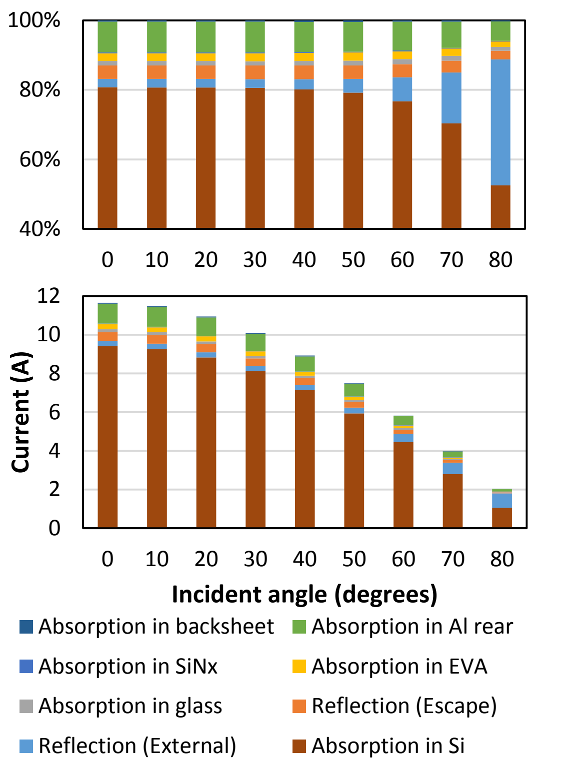

Figure 4: Optical loss analysis of the baseline module as a function of zenith angle shown as a (top) percentage of total available current and (bottom) absolute cell current.

The angular dependent losses showed that, as expected, the most significant impact of the zenith angle was an increase in the percentage of loss due to reflection from the front surface of the glass.

3. FURTHER APPLICATIONS

The previous section described the simulation of baseline modules. This section demonstrates how the simulation input parameters can be varied to assess the impact of different properties.

3.1 Spacing between cells

The space between the cells in a module is an important region to optimize. This area does not contain a solar cell absorber, however, it is well known that light incident on these areas can be collected via reflection from the backsheet and internal light trapping beneath the glass. The effectiveness of this process is very dependent on the properties of the backsheet. There are many options for material to use, some designed for high efficiency and others intended to create an appealing look (i.e. all black modules).

An extremely important property of a backsheet is the ability to scatter light. Here we model this using a simple Lambertian function in which the fraction of light scattered in a Lambertian fashion is defined by a value that does not change with wavelength. The impact of this on the collection of current as a function of the spacing between the cells is shown in Figure 5. In this experiment the spacing between cells for the baseline module was varied along with the Lambertian fraction of the rear interface (i.e. the backsheet).

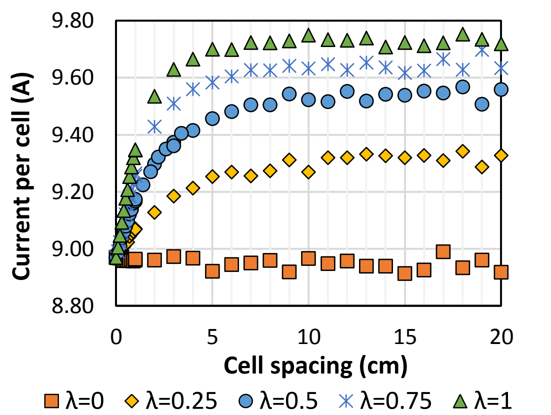

Figure 5: Current produced under normally incident light by a module unit cell as a function of cell separation, simulated for the baseline module using a backsheet with various values of Lambertian fraction.

The simulated values of module current for different white space properties (Figure 5) demonstrate the strong impact on module performance of these regions. With no lambertian scattering and normally incident light the module current sees no change as the total area is increased. This occurs as no light incident on those areas is able to spread sideways onto the cell. By comparison the samples with lambertian reflection show increasing total current due to the collection of light from outside the cell area. As the spacing is further increased the current saturates as the longer path to the cell results in other losses dominating. Interestingly the model predicts that for the inputs used in this work, collection of light can occur from as far away as 10cm.

3.2 Optimisation of front surfaces

It is common for device engineers to optimize the cell design based on electrical performance measured using an IV tester in which the layer above the cell is air. However, the end module product includes layers of glass and EVA above the cell that create the possibility of internal light trapping. To demonstrate this impact we simulated the case of front surface AR coating thickness optimization. Figure 6 plots the normalized module current, under normally incident light, for three different surface morphologies as a function of the thickness of the front AR coating (SiNx).

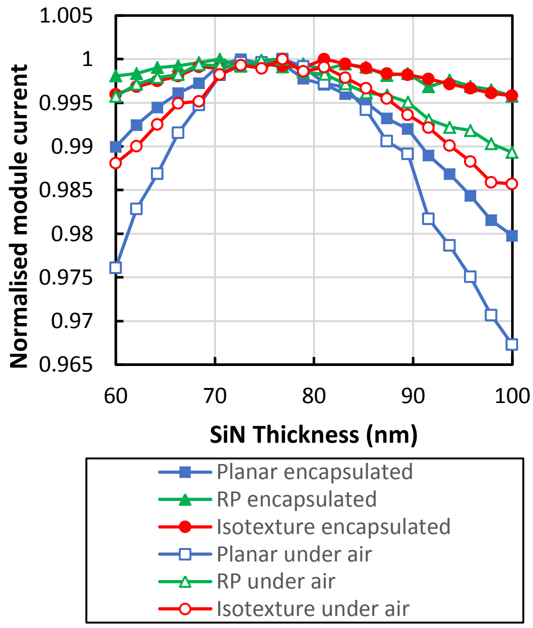

Figure 6: Normalised current produced under normally incident light as a function of solar cell front AR coating thickness, shown for different surface morphologies under air and under encapsulation.

The impact of the front side AR coating film thickness on the Isc of a cell is significantly reduced when that cell is encapsulated. This effect is greatest for samples with either random pyramid (Figure 6 triangles) or isotexture (Figure 6 circles) morphologies on the surface. In those cases the current varies less than 5%rel for a range of thicknesses from 60 nm to 100 nm. In all cases the optimal thickness was found to be 75 nm. This provides just one example of how encapsulation should be considered in cell design. In this case the optimal point was the same, but the sensitivity to the value was reduced under encapsulation.

4. CONCLUSIONS

This paper investigated the application of ray tracing to the optical analysis of solar modules. Specifically it presented a new tool from PV Lighthouse capable of rapidly solving many thousands of rays through a series of optical layers joined with textured, thin film interfaces. As an example a baseline module was described and compared to the performance of current commercial modules and cells as reported in manufacturer datasheets.

It was shown that the simulation approach is capable of reproducing the performance of such modules and that this then allows a detailed loss analysis of the optics to be determined. Furthermore the impact of the number of rays used within the simulation on the errors in the final result was presented.

Finally the paper demonstrated a number of example applications of module simulations. These included determining the module performance as a function of cell spacing, rear surface lambertian fraction and optimization of front surfaces under encapsulation.

Future work on the module ray tracer will seek to advance the approach by incorporating metal contacts as well as presenting more detailed validation through comparisons with experimentally measured datasets.

5 REFERENCES

[1] https://www.pvlighthouse.com.au
[2] K.R. McIntosh and S.C. Baker-Finch, “OPAL 2: Rapid optical simulation of silicon solar cells,” in *38th IEEE PVSC*, Austin, 2012, pp. 265–271.
[3] Keith R. McIntosh, Thomas G. Allen, Simeon C. Baker-Finch and Malcolm D. Abbott, "Light trapping in isotextured silicon wafers", *43rd IEEE PVSC*, Portland, 2016
[4] Keith R. McIntosh, Malcolm D. Abbott, Matt Edwards, Rhett Evans and Yu Yao, "Optical evaluation of multi-wire modules", *32nd EU-PVSEC*, Hamburg, 2016
[5] http://www.enfsolar.com/pv/panel
[6] K.R. McIntosh, J. Cotsell, J. Cumpston, A. Norris, N. Powell and B. Ketola, “An optical comparison of silicone and EVA encapsulants for conventional silicon PV modules: A ray-tracing study,” *34th IEEE PVSC*, Philadelphia, pp. 544–549, 2009.
[7] S. Duttagupta, F. Ma, B. Hoex, T. Mueller and A. Aberle, “Optimised antireflection coatings using silicon nitride on textured silicon surfaces based on measurements and multidimensional modeling,” *Energy Procedia* 15(0), pp. 78–83, 2012.
[8] M.A. Green, “Self-consistent optical parameters of intrinsic silicon at 300K including temperature coefficients,” *Solar Energy Materials and Solar Cells*, vol. 92 (11), pp. 1305–1310, 2008.
[9] A. Fell *et al*., "Input Parameters for the Simulation of Silicon Solar Cells in 2014," in *IEEE Journal of Photovoltaics*, vol. 5, no. 4, pp. 1250-1263, July 2015.
[10] Pietro P. Altermatt, “Models for numerical device simulations of crystalline silicon solar cells—a review”, *Journal of Computational Electronics*, September 2011, 10:314